# Modification of Lu's (2005) high pressure model for improved high pressure/high temperature extrapolations. Part I: modeling of platinum at high pressure/high temperature

Jean-Marc Joubert, Jean-Claude Crivello, G. Deffrennes

# Modification of Lu's (2005) high pressure model for improved high pressure/high temperature extrapolations. Part I: modeling of platinum at high pressure/high temperature

Jean-Marc Joubert[1], Jean-Claude Crivello[1], G. Deffrennes[2]

[1]Univ Paris Est Creteil, CNRS, ICMPE, UMR 7182, 2 rue Henri Dunant, 94320 Thiais, France

[2] CEA, DAM, VALDUC, F-21120 Is-sur-Tille, France

e-mail address of corresponding author: joubert@icmpe.cnrs.fr

**Abstract**

Calphad description at high pressure is a very important topic. Several models have been proposed in the literature. The model proposed by Lu *et al.* (X.-G. Lu, M. Selleby and B. Sundman, Comput. Coupling Phase Diagr. Thermochem., 29 (2005) 49-55) is very convenient in many aspects. But it has been criticized for giving unphysical extrapolations in certain conditions. We show that this model is indeed suitable if additional constraints on several parameters are made in order to obtain consistent extrapolations when both high pressure and high temperature are considered. This revised model will be applied to the complete description of the Os–Pt system. In this first part, the thermodynamic assessment of platinum in both solid and liquid phases is presented. The use of DFT and phonon calculated data provided in the present work will be shown to be useful for the thermodynamic assessment. A consistent description of Pt at high pressure and temperature (equation of state) including the liquid phase and phase diagram is given for the first time.

Keywords: Calphad, model, EOS, DFT, platinum, high pressure

## 1. Introduction

Modeling of both thermodynamic properties and phase diagrams at high pressure is very important not only for geological applications. It is also needed for the description of materials under thermomechanical stress, impact or explosion, for the prediction of molar volume... High pressure properties are obviously also strongly related to the basic physics of the materials. The models used must combine the possibility to reproduce well the data, the ease of use and accurate extrapolations. There exist different high pressure models in the literature that can be used in the frame of the Calphad methodology: Mie-Grüneisen (1912), Murnaghan (1944), Birch-Murnaghan (1947), Refs. [1-8]. However, there is no consensus about which is preferable.

Among them, the model by Lu *et al.* [2] has had indisputable achievements. It is particularly interesting because it has been implemented in the Thermo-Calc software, it is relatively easy to handle, it can treat any phase, solid or liquid, stable or metastable and it follows the Calphad formalism in its extrapolation possibilities to multi-component systems. However, it has been criticized for leading to sometimes erroneous extrapolations at high pressure and/or temperature (negative entropy and specific heat). We will describe the limitations of this model in more detail and their origin will be investigated. Solutions will be proposed in order to avoid the problems of extrapolation. It will be finally demonstrated that it may be used safely with the proposed modifications and that, in most cases, it should be preferred as being simpler, easier to handle and because it is better adapted to the frame of the Calphad method, to the description of complete systems and to the extrapolation to multicomponent systems.

As an application, the example of platinum at extreme pressure and temperature will be detailed in the present paper. A thermodynamic assessment of the available experimental data together with

calculated data obtained in this work will be described. In the second part of this study [9], this model will be applied to the complete description of Os–Pt binary system .

## 2. Description of Lu's model

In high pressure models, the Gibbs energy is described with an additional contribution taking into account the temperature and pressure dependence of the volume:

$$G = G(T, p_0) + \int_{p_0}^{p} V(T, p')dp' \qquad (1)$$

In Lu's model [2], the volume is described as a function of pressure using the Grover equation, itself derived from the Murnaghan model (see the original paper for the complete description and derivation of the equations). Finally, the volume is calculated as a function of temperature and pressure in Equation 9 of Lu's paper adapted here with other notations:

$$V(T,p) = V_C E_1^{-1}\left[E_1\left(\frac{V_0 \exp(V_A)}{V_C}\right) + (p - p_0)V_K \exp\left(-\frac{V_0 \exp(V_A)}{V_C}\right)\right] \qquad (2)$$

where $E_1 = \int_z^{\infty} \frac{\mathrm{e}^{-x}}{x}\mathrm{d}x$ is the exponential integral function and $E_1^{-1}$ its inverse function. The model is fully implemented in Thermo-Calc software using the dedicated functions.

- $V_0$: a constant equal to the molar volume at a reference temperature (here 0 K) and 1 bar
- $V_A(T)$: integrated volume thermal expansion such as

  $$V(T, p_0) = V_0 \exp(V_A) \qquad (3)$$

  If described as:

  $$V_A = aT + bT^2 + cT^3 \qquad (4)$$

  then the average linear thermal expansion is:

  $$\alpha = (a + 2bT + 3cT^2)/3 \qquad (5)$$
- $V_C(T)$: pressure dependence of the bulk modulus ($B$)
- $V_K(T)$: isothermal compressibility at 1 bar

Among these functions, $V_A$, $V_K$ and $V_C$ are temperature dependent, though the use of temperature dependence for $V_C$ is not recommended. They can be optimized using the following data which are generally available from experiments:

- molar volume as function of temperature at ambient pressure makes it possible to determine $V_0$ and $V_A$
- thermal expansivity as a function of temperature is related to $V_A$
- molar volume as function of pressure at room temperature is related to $V_0$, $V_K$ and $V_C$
- bulk modulus as a function of temperature is related to $V_K$

The data used can be not only experimental but also calculated either from first principles calculations ($V_m = f(p)$) or by phonon calculations ($V_m$, α, $B = f(T)$), for example, in the quasiharmonic approximation.

## 3. Problems with Lu's (2005) model

### *3.1 Reported problems*

Soon criticisms about this model appeared in the literature. The main criticism is that the model yields nonphysical extrapolated values of $C_p$ and entropy. As an example, in Fig. 1, the $C_p$ of *bcc* Fe is calculated from the assessment of Lu *et al.* [2]. The figure shows that negative $C_p$ are obtained at high temperature at pressures above 100 GPa.

Brosh *et al.* [5] analyzed the problem as being due to an 'incompatibility' between the SGTE description of the $C_p$ and the Mie-Grüneisen equation. By second derivation of Eq. (1), one may obtain the $C_p$ at high pressure.

$$C_p = -T\left(\frac{\partial^2 G}{\partial T^2}\right)_p = C_p^{SGTE} + C_p^{model} \quad (6)$$

The $C_p$ is therefore the sum of the low pressure $C_p$ coming, for example, from the SGTE description and a contribution given by the model at high pressure.

Brosh *et al.* assume that the contribution of the second term at high temperature (above the ambient pressure melting point) is necessarily negative. Therefore, according to these authors, in order to avoid that the overall $C_p$ becomes negative at high temperature when pressure (and therefore melting point) is raised, then the first term should increase strongly as a function of temperature above the ambient pressure melting point of the element. This disagrees with the so-called SGTE approximation [10, 11] tending to have constant $C_p$ at high temperature above the melting point of the elements as shown in Fig. 1. This is what the authors call an 'incompatibility' between the SGTE database and high pressure models.

The validity of the assumption of Brosh *et al.* is not obvious because it can be imagined as well that the high pressure contribution to the $C_p$ should not be negative and that the Mie-Grüneisen model itself badly reproduces the features at high pressure. So, it is not a question of incompatibility, it is rather a question of defining what should be the $C_p$ above the melting at low pressure and what should be the contribution to the $C_p$ at high pressure. It is not proven that this second contribution should be high and negative.

One can see, for example, that negative $C_p$ can be obtained with the model of Lu at 200 GPa at temperatures below the ambient pressure melting point of *bcc* Fe. The problem can therefore not be caused by the term $C_p^{SGTE}$ in Eq. (6) since, at this temperature there is no other option than sticking to the consistently evaluated $C_p$ of the *bcc* phase. If one wants to avoid negative $C_p$, then one should work on the contribution to the $C_p$ of the high pressure model itself.

### *3.2 Analysis of the problem*

In order to discover the origin of the problem, we conducted several simulations using Lu's model. Calculated data will be reported for $C_p$ but note that the same tendency is also observed for entropy (*i.e.* when negative $C_p$ is calculated, negative entropy is also calculated). The effects of the compressibility and the thermal expansion are examined separately. The simulations for a phase without thermal expansion show that the compressibility itself is not a problem. Indeed, the $C_p$ calculated up to 1000 GPa, whatever the compressibility, is the same as the low pressure $C_p$. This is also in contradiction with the analysis of Brosh *et al.* [5] *i.e.* the Gibbs energy contribution at high pressure calculated from the model does not bring any negative contribution to the $C_p$ and there is therefore no need for the low pressure $C_p$ to increase above the melting point.

Let's now examine the effect of thermal expansion for an uncompressible phase. The results are presented in Fig. 2. Negative $C_p$ is definitely observed at high pressure and temperature. This can be understood by writing the following equations from Eq. 1 for an uncompressible phase in which $V$ does not depend on $p$:

$$G = G(T,p_0) + \int_{p_0}^{p} V(T,p')dp' = G(T,p_0) + \int_{p_0}^{p} V(T)dp' = G(T,p_0) + V(T)(p-p_0) \quad (7)$$

$$C_p = -T\frac{\partial^2 G}{\partial T^2} = C_p^{SGTE} - T(p-p_0)\frac{\partial^2 V}{\partial T^2} \quad (8)$$

From this equation, there is actually a negative contribution. It is not directly caused by the thermal expansion (proportional to $\frac{\partial V}{\partial T}$) but rather by the increase of thermal expansion as a function of

temperature (proportional to $\frac{\partial^2 V}{\partial T^2}$). This can be checked in Fig. 2 where a constant thermal expansion is used without causing a significant $C_p$ decrease at high pressure.

Eq. 8 has been derived for the specific case of an uncompressible phase for the sake of simplicity. A more general expression can be obtained, without making any kind of assumption, by using the Maxwell equation (as quoted in Ref. [10]):

$$\left(\frac{\partial C_p}{\partial p}\right)_T = -T\left(\frac{\partial^2 V}{\partial T^2}\right)_p \qquad (9)$$

It indicates as well the $C_p$ decreases when pressure is raised if $\frac{\partial^2 V}{\partial T^2}$ is positive.

Practically, at ambient pressure, $\frac{\partial^2 V}{\partial T^2}$ is always positive and may be very large for several elements as obtained experimentally from ambient pressure measurements of volume or thermal expansion as a function of temperature (see in Ref. [12] the assessment of the thermal expansion of many different elements). Whatever model reproducing the available experimental data should therefore reproduce this negative contribution to the $C_p$ at low pressure. Note that this is not model dependent, this contribution being inherent to the data. The problem is coming from this negative term. If kept constant as a function of pressure, it will have a dramatic influence on the $C_p$ when calculated at both high pressure and temperature. It is therefore compulsory that it decreases with pressure and this has not necessarily been considered in the models.

First, thermal expansion or high temperature volume data are rarely known at high pressure, so a fit of the pressure dependence of thermal expansion coefficients cannot be performed. For few systems in which thermal expansion has been measured at high pressure, as expected, the slope of thermal expansion as a function of temperature and even thermal expansion itself is observed to decrease (see *e.g.* MgO and $MgSiO_4$ in data reproduced in Refs. [1] [4]).

Second, such a fit should be allowed by the model. This is indeed the main problem with Lu's model: the thermal expansion controlled by the parameter $V_A$ (Eq. 4) is not made pressure dependent while it should. The uncontrolled behavior of $\frac{\partial^2 V}{\partial T^2}$ at high pressure, especially if thermal expansion increases as a function of temperature, even more if the second derivative of thermal expansion is positive and high (see *e.g.* the example of Mo in Ref. [12]), is responsible for the predicted negative $C_p$ when high pressure and high temperature are combined.

## 4. Possible solution

It is always possible to fit the volume as a linear function of temperature (no curvature in the volume curve or constant thermal expansion). As can be inferred from Eq.9, it would allow to maintain a constant $C_p$ as a function of pressure. This would however be a crude approximation resulting in a poor description of the data and therefore of the thermodynamic properties. Another option is to keep a good description of the low pressure thermal expansion data but make the thermal expansion constant in the high pressure regime. This is possible by using an exponential term $\exp\left(-\frac{p}{p_{\text{cut}}}\right)$ intended to damp the terms in $T^2$ and $T^3$ in Eq. 4 at high pressure.

A value of the cut-off pressure $p_{\text{cut}}=10^9$ Pa gave satisfactory results. Additionally, it is possible to make the thermal expansion decrease at high pressure by applying a similar exponential term on the $T$ term as well. This second cut-off pressure ($p_{\text{cut'}}$ typically around $10^{11}$ Pa) can be adjusted from the data when existing (for example volume at both high pressure and temperature) or set arbitrarily.

We propose such an equation instead of Eq. 4:

$$V_A = aT\exp\left(-\frac{p}{p_{\text{cut'}}}\right) + bT^2\exp\left(-\frac{p}{p_{\text{cut}}}\right) + cT^3\exp\left(-\frac{p}{p_{\text{cut}}}\right) \qquad (10)$$

At low pressure, this results in a linear thermal expansion equal to:

$$\alpha = (a + 2bT + 3cT^2)/3 \qquad (11)$$

identical with the original model.

The intermediate pressure limit, typically above $p=p_{cut}$ is:

$$\alpha = a/3 \qquad (12)$$

While, at high pressures ($p>>p_{cut'}$), the thermal expansion converges to zero.

It is also found that cross correlations between thermal expansion and compressibility parameters have a contribution to the $C_p$, although to a lesser extent than the coefficients of thermal expansion. This may be seen from the thermodynamic identity:

$$\left(\frac{\partial \alpha}{\partial p}\right)_T = \frac{1}{\kappa^2}\left(\frac{\partial \kappa}{\partial T}\right)_p \qquad (13)$$

Therefore, it may be recommended to damp also, with the same exponential term, the temperature dependence of $V_K$:

$$V_K = a + bT\exp\left(-\frac{p}{p_{\text{cut}}}\right) + cT^2\exp\left(-\frac{p}{p_{\text{cut}}}\right) + dT^3\exp\left(-\frac{p}{p_{\text{cut}}}\right) \qquad (14)$$

Eq. 2 remains valid provided the term $V_0\exp(V_A)$ is used. Note that it represents $V(T)$ only at low pressure but no longer at high pressure since $V_A$ is now pressure dependent.

## 5. Application

We present here an application of the modified model to the description of platinum. This system has been chosen because a lot of data is available up to very high pressure. It is also important because platinum may be used as a pressure standard in high pressure diffraction experiments. Both *fcc* and liquid phases will be described allowing a calculation of the pressure–temperature phase diagram.

### *5.1. Selection of data*

#### 5.1.1. *fcc* phase

The molar volume and thermal expansion data have been thoroughly reviewed by Arblaster in different publications [13, 14]. These assessed data will be used as experimental data for the present assessment. It offers the advantage of a proper correction of the different temperature scales used in the older literature, a proper conversion from kX to Å when appropriate, a careful selection of the most accurate data and an assessment along the complete temperature range. Anyhow, there is no significant discrepancy in the literature, except perhaps the data of Refs. [15-17]. These data have been obtained in the frame of a study of the liquid volume with an optical measurement which is probably less reliable than high temperature diffraction results. Several chosen significant data are reported in Table 1 and will be plotted for comparison.

Compressibility data at room temperature are available from different authors [18-21]. In general, the agreement is very good between the different datasets. We note the availability, for this system, of data at both high pressure and temperature [19, 20, 22] which is very important in the frame of this work. More recent data by Huang *et al.* [23] have been found to be not only inconsistent with the other authors but also self-inconsistent. They were not considered in the present work.

Shock wave data are available in the form of Hugoniot plots and are essentially compatible with each other [24-27]. In the three Refs. [25], [24] (converted in Ref. [27]) and [27], they have been converted into isotherms at room temperature and compare very well with cold compressibility curves. These converted data will be used in the optimization. The advantage of shock wave data is the possibility

to extend the description up to extremely high pressure not reached with conventional compressibility measurements. The adiabatic bulk modulus as a function of temperature measured by sound velocity [28] has been converted into isothermal bulk modulus.

Density Functional Theory data (DFT) is also available for Pt. Both Refs. [29, 30] use Local Density Approximation (LDA) functional in quasiharmonic phonon calculations. As usual for DFT data, it is difficult to reproduce exactly the experimental volume which causes problems if one wants to use the data in the optimization. An empirical correction is needed not only at low temperature (to compare with the cold compression curve) but also at high temperature to account for anharmonic phonon-phonon and electron-phonon contributions.

New DFT data have been obtained in the frame of the present work. Details of the calculations (classical DFT and phonon calculations in quasiharmonic approximation) can be found in our previous papers [31]. Calculations of the molar volume, thermal expansion and bulk modulus at zero pressure and volume as a function of pressure at 0 K have been obtained. In order to have the best agreement between the equilibrium volume and the experimental one, the three functionals PBE, PBEsol and LDA were tested [32, 33]. Compared to experiments, PBEsol gives far better agreement on the volume than the other functionals. As a classical scheme, PBE overestimates while LDA underestimate the volume (see the comparison in Supplementary Data). With PBEsol, the volume at low temperature and the bulk modulus is perfectly reproduced. No significant difference is observed between the DFT volume and that obtained from the phonon calculation ($9.042 \times 10^{-6}$ vs $9.062 \times 10^{-6}$ $m^3$/mol). The thermal expansion is slightly overestimated (it is a bit better with LDA) which makes the agreement with the experimental volume and bulk modulus less good at high temperature. Overall, with PBEsol the comparison with experimental data is very good but not enough to be used in the frame of the thermodynamic optimization. DFT data is also not really needed when exists trustful experimental data. It will be shown on the graphs for comparison only.

More interesting is the derivation of both volume and thermal expansion at both high pressure and temperature. For this, the following procedure was adopted. Energy-volume relationships were obtained at different temperatures up to 3000 K from phonon calculations. The calculated data was fitted to a $4^{th}$ degree polynomial. The pressure as a function of volume obtained by derivation is then described as a $3^{rd}$ degree polynomial. The equation is solved in order to obtain the volume as a function of pressure at different temperatures. A numerical derivation as a function of temperature can then be made to obtain the thermal expansion at different pressures.

### 5.1.2. liquid phase

Molar volume as a function of temperature is available from different authors below (undercooled liquid) and above the melting point. One must stress the extreme difficulty of such measurements. Three groups of datasets can be distinguished. Stankus and Khairulin [34] and Mehmood *et al.* [15] have higher values, Gathers *et al*. [35, 36], Hixson and Winkler [37], Ishikawa *et al.* [38] and Paradis *et al.* [16] have intermediate values and, finally, Klotz and Plevachuk [17] have the lower values. Arblaster [39] stated that the intermediate values for the volume change at the melting point should be preferred because they better agree with the measurement of the melting point as a function of pressure (the two depend on each other through the Clausius-Clapeyron relationship). The data of Ishikawa *et al.* and Paradis *et al.* are particularly valuable because they extend well below the melting point. In addition, the measurement of the size of a levitated droplet is more accurate than the measurement of a wire diameter used by other authors [15, 35-37]. Among the two datasets, the one of Paradis *et al.* should be given a larger weight due to a better accuracy (J.F. Paradis, personal communication). The extension to extremely high temperature in the data of Gathers *et al*. [35, 36] and Hixson and Winkler [37] has been considered but the disagreement is significant.

The melting curve was studied by different authors. The most complete experimental works are those of Errandonea [40] for pressures up to 28 GPa and Anzellini *et al.* [21] for pressures up to

84 GPa. They agree very well with previous experimental work by Mitra *et al.* [41] and Vereshchagin and Fateeva [42] and theoretical predictions by the so-called Z method [21, 43, 44] or by molecular dynamics [45, 46]. The lower values of the melting point of Ref. [47] and [48] were not considered. Note that Ref. [44] predicts a randomly disordered hexagonal close-packed phase above 50 GPa in equilibrium with the liquid. This has been confirmed neither experimentally nor by other calculations and will not be considered in the present assessment. Finally, the bulk modulus has been derived from sound velocity measurements as a function of temperature at extremely high temperature [37].

#### 5.1.3 Previous assessments of the system

Several equations of state for *fcc* platinum are available in the literature [18-20, 22, 25, 27, 30, 49-51]. No model has been proposed for the liquid and no Calphad-type assessment is available in the literature except in the following reference, in Chinese, presenting the modeling of the *fcc* phase (no liquid) using the Debye-Grüneisen model [52]. It is also interesting to mention the description by Karbasi *et al.* [50] using the model of Brosh *et al.* [5].

### *5.2 Results*

All the parameters were optimized using the Parrot module of Thermo-Calc. The *fcc* phase was optimized first. A good agreement was obtained with our model using a limited number of parameters. The cold compression curve allows to optimize $V_0$, bulk modulus and pressure dependence of the bulk modulus while thermal expansion terms were refined from the low pressure volume and thermal expansion function of temperature. For the compressibility, in the low pressure range (0-90 GPa), all the SRXD data are in excellent agreement and were used simultaneously. For higher pressure, only shock wave data exists. The optimization of the data of McQueen *et al.* [24] were preferred because they better match the SXRD data. It is an intermediate between the data of Morgan [25] and Holmes *et al.* [27] extending to the highest pressures.

Then, the data combining high pressure and temperature were optimized. As mentioned before in the theoretical development of the model, in addition to the cut-off pressure for the temperature dependent terms for $V_K$ and terms in $T^2$ and $T^3$ for $V_A$ ($p_{cut}$=$10^9$ Pa), it was found necessary to introduce a second cut-off pressure ($p_{cut'}$) for the term in $T$ for $V_A$ corresponding to the constant thermal expansion. This cut-off pressure could be refined using the experimental data and our own DFT data at high temperature and a very good agreement is obtained with this single parameter both on the presentation of volume as a function of temperature at high pressure, and volume as a function of pressure at high temperature. This not only proves that thermal expansion should decrease as a function of temperature but also confirm the relevance of our exponential term to achieve this.

Hugoniot data cannot be used directly in the optimization. They can, however, be calculated after the model is established. The comparison shows a relative agreement that can be explained by an underestimation of the thermal expansion at extremely high pressure. A better agreement of the Hugoniot was obtained by Karbasi *et al.* [50] using the model of Brosh *et al.* [5].

Figs. 3 to 8 present the results with a comparison with experimental data. In Fig. 5, the low temperature range is evidently not described by our simple model of thermal expansion.

The liquid was then modeled with a limited set of parameters and parameters of the *fcc* phase fixed. $V_0$ and thermal expansion were refined from the volume as a function of temperature. Care was taken in order to have the volume of the liquid always higher than that of the solid. The volume of Gathers *et al.* (at 0.3 GPa) [35, 36] is larger than that of Hixson and Winkler [37] which should evidently not be the case. On the other hand, none of these two datasets is compatible with that of Paradis *et al.* [16] close to the melting point. A compromise was obtained between the data of Paradis *et al.* that were preferred because it is more accurate and that of Hixson and Winkler around

4000 K which allows also to reproduce the data of Gathers *et al.* around 7000 K. The melting temperature as a function of pressure was successfully described at the same time of the bulk modulus function of temperature. This confirms the good estimation of the volume change at the melting point and its temperature and pressure variation. The liquid has a lower bulk modulus than the solid but becomes stiffer with the pressure. The results are presented in Figs. 9 to 11 and the volume function of pressure for which no data is available is shown in Fig. 4a.

Above 150 GPa melting can no longer be described. This is because the *fcc* phase becomes stable over the liquid at very high temperature, even at low pressure, due to unconsidered variation of the $C_p$ of the *fcc* phase at high temperature as illustrated in Fig.12. Except this anomaly caused by the SGTE description of the *fcc* phase that will be discussed later, no strange behavior is observed up to extreme pressures demonstrating the efficiency of our correction to Lu's model.

Table 2 presents the refined optimized parameters for the two phases.

## 6. Discussion

### *6.1 Other models*

As observed in the introduction, many models are available in the literature. We will limit our comparison to the most recent ones [5-7, 51]. These models are based on the quasi-harmonic approximation, the Debye-Grüneisen model, or the modeling of phonon frequencies, respectively. They offer very sound and complete approaches encompassing a closer relation to the physics and a superior use of DFT data and phonon calculations.

However, as a consequence of their link to the DFT or phonon calculation, most of them are limited to the only phases that can be calculated by these methods *i.e.* crystalline and stable phases. Unstable structures that have, for example, imaginary phonon frequencies or the liquid phase cannot be described using these models. Additionally, they do not use the SGTE description of the pure elements which is a severe limitation if one wants to implement pressure models in already assessed systems using the SGTE description.

These two features limit severely their applicability as regards the extension to the calculation of complete phase diagrams (including liquid) and the extension to multicomponent systems involving metastable (unstable) end-members as usual for the Calphad technique.

As an exception, Brosh's (2007) model [5] has been designed to follow SGTE at low pressure and converges to the quasi-harmonic model at high pressure. It is therefore physically correct and has had undeniable achievements including for platinum, as we already mentioned [50], and even with the modeling of binary systems (Al–Si [5], Fe–C [53]).

But, all the models, including Brosh's, because of their complexity and the high number of parameters they use, are not adapted to systems for which only few data exist, or sometimes no data at all as it may be the case for metastable phases. Anticipating and fixing values, in such cases, may be difficult since the meaning and the effective influence of the model parameters on the volume and its derivative is difficult to comprehend. They may also neither be programmed nor used with the optimization modules of thermodynamic software packages because of their complexity. As an example Karbasi *et al.* [50] write that Cr and Ni could not be treated with Brosh's model due to the scarcity of data.

### *6.2 Advantages of Lu's model*

In comparison, the advantages of Lu's (2005) model are numerous. First, it is simple to use and the meaning and the influence of each parameter on the physical quantities like the volume or its

pressure and temperature derivatives is easy to understand. As a consequence, it is uncomplicated to limit the number of parameters, or fix some, depending on the amount of data. It is fully compatible with SGTE. But it does not prevent the use of DFT and phonon calculation, as shown here, and as will be shown in the second part of this study [9].

It is fully adapted to the Calphad methodology. It is phenomenological like the Calphad method is. This includes the extrapolation possibilities to describe complete or non-complete solid solutions [54]. It may be used for stoichiometric or non-stoichiometric compounds within the sublattice model, like for example to describe interstitial solid solutions [31]. It can be used for any kind of phase, crystalline or not (solid or liquid), stable or not (not stable end-members, pure elements in non-stable structures). Of course, assumptions should be made to describe metastable phases when no data exist. This will be shown in Part II of this paper. The functions are compatible with the Calphad mixing formalism, they can be extended as a function of composition using excess terms similar to other (energetic) mixing parameters. This means that complete phase diagrams can be described and that predictions made in the frame of classical Calphad extrapolations can be made by combining systems. Another advantage is that it is also fully implemented in Thermo-Calc so that there is no need to develop an additional code for its application.

Lu's phenomenological model is therefore probably better than other more physical model for the construction of Calphad databases. The only drawback of the model was the wrong extrapolation of entropy and $C_p$ at high temperature and pressure. This paper has shown that this problem was essentially due to the fact that thermal expansion (and to a lesser extent temperature dependence of the compressibility) was left uncontrolled at high pressure. We have also shown that the problem can be easily solved.

We obtained a complete description of the Pt system including the liquid phase with a very good description of the available data. The model is simple and easily transferrable to any other system. It can also be extrapolated to higher order systems as will be shown for Os–Pt system in the second part of this study [9].

### *6.3 Problem of high temperature heat capacity from SGTE*

More than Lu's model, the SGTE database should be criticized. It is not adapted to the use of high pressure models. This is for two different reasons. First, the lattice stabilities are not adapted to a raise of the melting point. For example, if liquid is suspended (or made less stable by the effect of pressure), *fcc* Os is stable against *hcp* phase at 5200 K without any reason. Second, the extrapolation of the $C_p$ of the solid above the melting point is wrongly done for many elements. In principle, the so-called SGTE approximation [10, 11] involving a convergence of the $C_p$ of the solid phase toward that of the liquid should be used. An examination of the PURE database [55] shows that, surprisingly, it is not the case for many elements. This was shown here for Pt. But this is also the case for Os and many other more common elements (Ta, Ti…). As a consequence, in our case, the uncontrolled $C_p$ of *fcc* Pt at high temperature causes the stabilization of this phase over the liquid at 11000 K and ambient pressure. Such high temperatures are rarely used in normal thermodynamic assessments, but they are common in the high pressure context as shown in Figs. 8 and 11.

At least the SGTE approximation should be used systematically. But, better, a revision of the PURE database is strongly recommended that would encompass the evaluation of sensible values for the solid above the ambient pressure melting point because they no longer characterize a metastable phase when pressure is raised. A very efficient way of doing this and solving this long standing problem (see *e.g.* the discussions on the $C_p$ of Al above its melting point [56-58]) would be the possibility to actually use high pressure in order to stabilize the solid phase and measure the $C_p$ above the normal melting point. This is probably difficult experimentally and, as far as we are aware, such measurements do not exist for metallic materials. This should be investigated, given the importance of such determination. A possibility would be to use shock wave measurements and Hugoniot curves

for such a purpose. Another option would be to impose a high temperature limit for the solid (but why not also for the liquid) equal to 3*R*. This is the expected limit at high pressure. So when the melting point raises with pressure the $C_p$ of the stable phase would naturally converge towards 3*R*. Finally, on may mention that our model can be used easily with 3rd generation databases.

*6.4 Remaining issues*

The presently modified model conveniently removes the negative contribution to the $C_p$ at high pressures and temperatures that was present in Lu's model. It allows a consistent description of the thermal expansion as a function of temperature when pressure is increased with a decrease of the slope around $p_{\mathrm{cut}}$ and a decrease of the thermal expansion itself around $p_{\mathrm{cut}'}$. This allows a good description of *p*–*V* curves at high temperature (Fig. 7). However, several anomalies remain. For example, a small increase of the bulk modulus as a function of temperature can be seen at $p$=$10^{11}$ Pa in Fig. 6. The slope decrease of the thermal expansion function of temperature at high pressure is not necessarily well controlled. One may see in Fig. 5 that thermal expansion is constant at 50 GPa while DFT calculations in the present and in other works [30, 59] show a remaining slope at this pressure. This may have an effect on the heat capacity. Indeed, at very high pressure, $C_p$ is expected to converge towards $C_V$ as seen in Ref. [59]. This can anyway not be the case in our model since, by construction, $C_p$ converges towards the ambient pressure SGTE value. The $C_p$ at high pressure is therefore essentially unchanged from the ambient pressure value which is at odds with the predictions of physically-derived models [59-61]. Also, a minimum of the $C_p$ is observed around 1 GPa which is an anomaly. Again, and as detailed in the previous paragraph, more attention should be given to the extrapolation of this parameter in the metastable range. It seems that Brosh's model [5] has more realistic behavior. But, these anomalies, because they relate to second derivatives, have a second order effects and therefore no significant consequences on volume and phase diagram descriptions. Evidently, extrapolations at extremely high temperatures and pressures should always be taken with care. But we believe that these anomalies have small effects compared to the experimental uncertainties on which the model is optimized.

## 7. Conclusion

A modification has been proposed to Lu's (2005) model to suppress the anomalous extrapolation of specific heat and entropy at high temperatures and pressures. With this modification, we have shown that such anomalies are not present in a typical system like platinum which has been described completely including the liquid phase. A model is always a tradeoff between accuracy, predictability and usability. Modified Lu's model is indeed so easy to handle compared to many other models that it should be considered again as a powerful tool in the Calphad approach, especially in the frame of assessment of multicomponent systems, including liquid, metastable end-members, and compounds for the development of complete and useful databases. The question of the validity of the SGTE database has also been raised. We will show an application to a binary system (Os–Pt) in the second part of this study [9].

## Acknowledgements

DFT calculations were performed using HPC resources from GENCI CINES (Grant A0080906175).

Table 1: summary of relevant data for the optimization of platinum (HT: High Temperature, HP: High Pressure, (S)XRD: (Synchrotron) X-Ray Diffraction, DAC: Diamond Anvil Cell).

| Phase | Data type | Range | Reference | Technique |
|---|---|---|---|---|
| *fcc* | *V-T* | 300-2000 K | [62] | HT XRD |
| | at $p$=$10^5$ Pa | | | |
| | | 300-2040 K | [34] | penetrating gamma radiation |
| | | 0-2041 K | [13] | assessment of experimental data |
| | | 1740-2042 K | [15] | optical measurement |
| | | 1790 -2030 K | [16] | optical measurement |
| | | 1788-2033 K | [17] | optical measurement |
| | α-*T* | 246-843 K | [63] | interferometry |
| | at $p$=$10^5$ Pa | | | |
| | | 10-1800 K | [64] | assessment of experimental data |
| | | 0-2041 K | [13] | assessment of experimental data |
| | | 293-2041 K | [14] | assessment of experimental data |
| | *V-p* | 0-268 GPa | [24] | shock wave |
| | at 300 K | | | |
| | | 0-680 GPa (293 K) | [25] | shock wave |
| | | 0-536 GPa | [27] | shock wave |
| | | 0-89 GPa | [18] | HP SXRD |
| | | 3-22 GPa | [19] | HP SXRD |
| | | 3-78 GPa | [20] | HP SXRD |
| | | 0-80 GPa | [21] | HP SXRD |
| | *B-T* | 300-1400 K | [28] | Sound velocity |
| | *V-T-p* | 300-1873 K | [19] | HT HP SXRD |
| | | 3-28 GPa | | |

| | | | | |
|---|---|---|---|---|
| | | 300-1900 K | [20] | HT HP SXRD |
| | | 3-78 GPa | | |
| | | 300-1600 K | [22] | HT HP SXRD |
| | | 21-42 GPa | | |
| | | 300-3150 K | [23] | HT HP SXRD |
| | | 0-90 GPa | | |
| | | 300-3000K | [21] | HT HP SXRD |
| | | 0-80 GPa | | |
| | Hugoniot | 0-260 GPa | [24] | shock wave |
| | | 0-680 GPa | [25] | shock wave |
| | | 0-680 GPa | [26] | shock wave |
| | | 0-660 GPa | [27] | shock wave |
| liquid | *V-T* | 2100-7300 K | [35, 36] | imaging, wire |
| | | (0.3 GPa) | | |
| | | 2040-2300 K | [34] | penetrating gamma radiation |
| | | 2040-5100 K | [37] | imaging, wire |
| | | 1690 (undercooled)-2210 K | [38] | imaging, levitation |
| | | 2040-2830 K | [15] | imaging, wire |
| | | 1740 (undercooled)-2340 K | [16] | imaging, levitation |
| | | 1818-2064 K | [17] | imaging, sessile drop |
| | | (undercooled) | | |
| | | 1700-2200 K | [39] | assessment of experimental data |
| | $T_m$-$p$ | 3-6 GPa | [41] | resistivity, anvil press |
| | | 0-4 GPa | [42] | optical, pressure vessel |
| | | 20-70 GPa | [47] | visual, DAC |
| | | 10-120 GPa | [43] | *ab initio* Z method |
| | | 4-28 GPa | [40] | optical, DAC |
| | | 0-350 GPa | [44] | *ab initio* direct and inverse Z method |
| | | 50-200 GPa | [45] | molecular dynamics |
| | | 0-80 GPa | [46] | molecular dynamics |

| | | | | |
|---|---|---|---|---|
| | | 13-35 GPa | [48] | optical, DAC |
| | | 12-122 GPa | [21] | *ab initio* Z method |
| | | 18-85 GPa | [21] | DAC, diffraction or temperature plateau |
| | *B-T* | 2040-5100 K | [37] | imaging, sound velocity |

Table 2: model parameters.

| Phase | Parameter | Value ($p$ in Pa, $V_0$ and $V_C$ in $m^3$/mol, $V_K$ in $Pa^{-1}$) |
|---|---|---|
| | $p_{\mathrm{cut}}$ | $1 \times 10^{9}$ |
| | $p_{\mathrm{cut}\prime}$ | $1.1051 \times 10^{11}$ |
| *fcc* | $V_0$ | $9.0204 \times 10^{-6}$ |
| | $V_A$ | $2.5978 \times 10^{-5}\, T \exp\left(-\frac{p}{p_{\mathrm{cut}\prime}}\right) + 1.3533 \times 10^{-9}\, T^2 \exp\left(-\frac{p}{p_{\mathrm{cut}}}\right) + 1.2683 \times 10^{-12}\, T^3 \exp\left(-\frac{p}{p_{\mathrm{cut}}}\right)$ |
| | $V_C$ | $1.6844 \times 10^{-6}$ |
| | $V_K$ | $3.6580 \times 10^{-12} - 1.0875 \times 10^{-16}\, T \exp\left(-\frac{p}{p_{\mathrm{cut}}}\right) + 5.6030 \times 10^{-19}\, T^2 \exp\left(-\frac{p}{p_{\mathrm{cut}}}\right)$ |
| liquid | $V_0$ | $9.4687 \times 10^{-6}$ |
| | $V_A$ | $2.9546 \times 10^{-5}\, T \exp\left(-\frac{p}{p_{\mathrm{cut}\prime}}\right) + 1.3976 \times 10^{-12}\, T^3 \exp\left(-\frac{p}{p_{\mathrm{cut}}}\right)$ |
| | $V_C$ | $1.4409 \times 10^{-6}$ |
| | $V_K$ | $5.0 \times 10^{-12} + 6.2266 \times 10^{-19}\, T^2 \exp\left(-\frac{p}{p_{\mathrm{cut}}}\right)$ |

Figures:

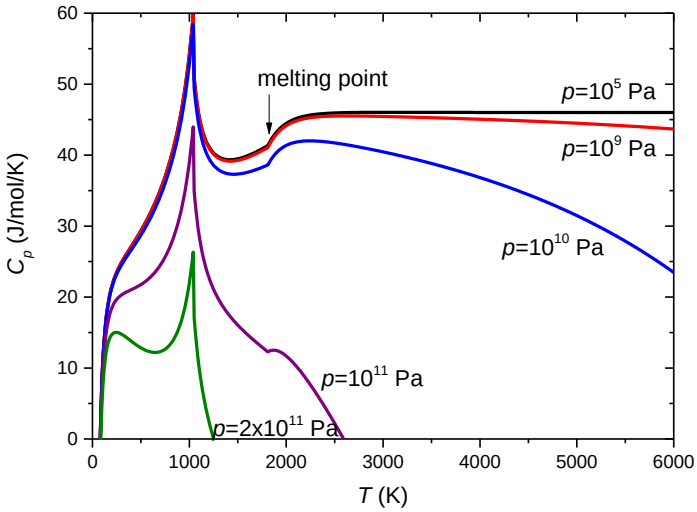


Figure 1: $C_p$ of *bcc* Fe calculated at different pressures from the assessment of Ref. [2].

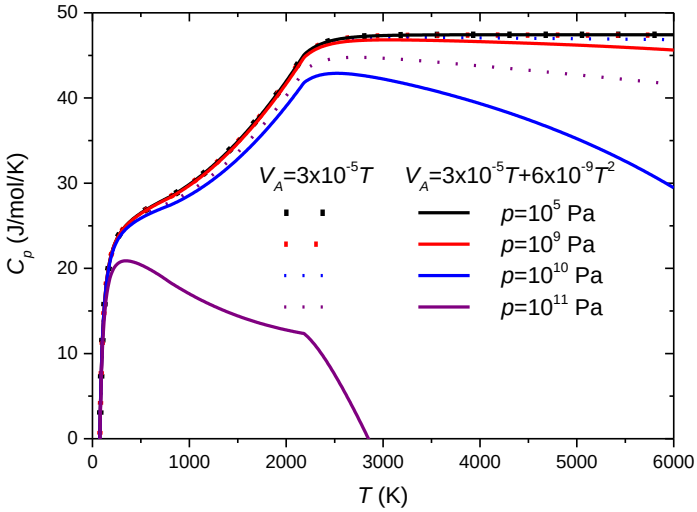


Figure 2: simulated $C_p$ at different pressures as a function of temperature for a hypothetical uncompressible element having different thermal expansion description.

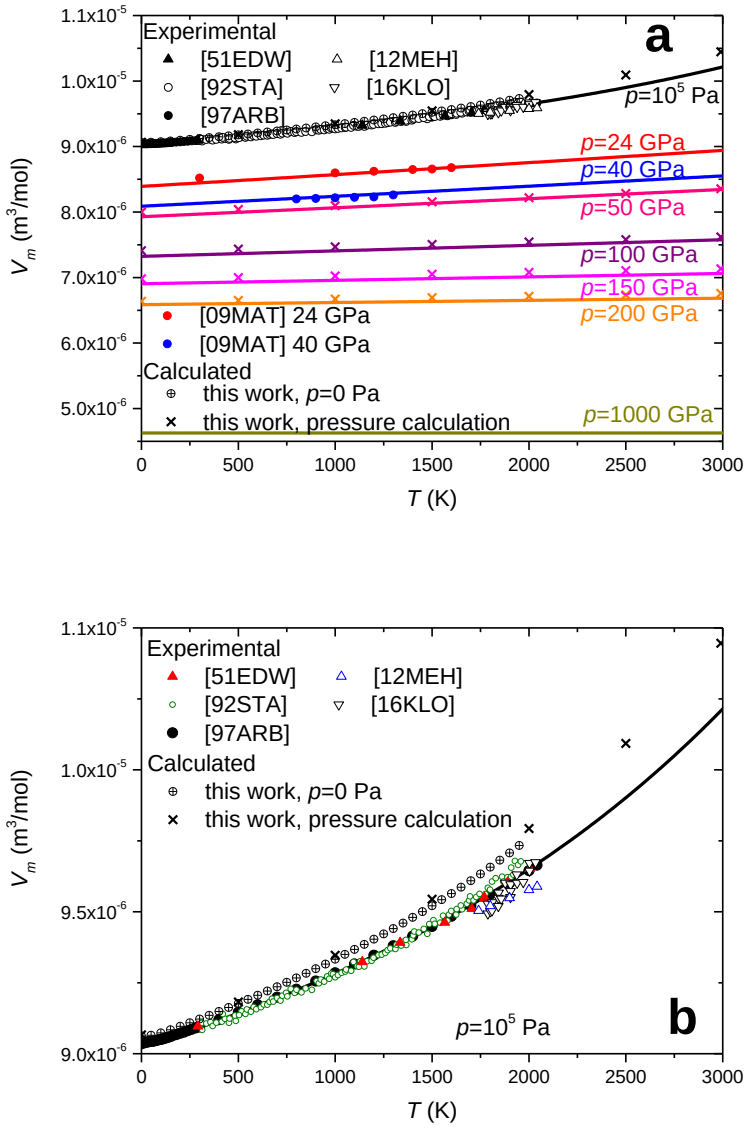


Figure 3: Molar volume of *fcc* Pt as a function of temperature at different pressures (full scale (a) and ambient pressure (b)). The experimental data are from Refs. [62] [51EDW], [34] [92STA], [13] [97ARB], [22] [09MAT] (at 24 and 40 GPa), [15] [12MEH] and [17] [16KLO]. Calculated data are obtained in this work from PBEsol DFT and phonon calculation at zero pressure and at different pressures (see text).

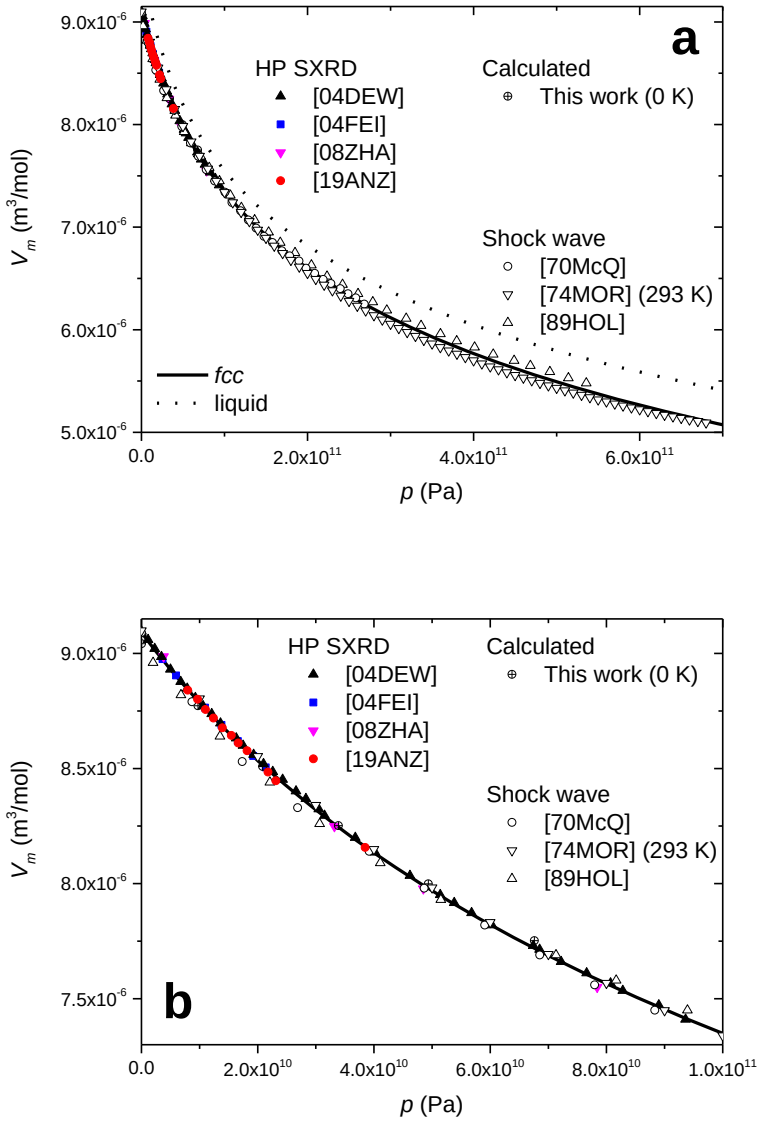


Figure 4: Molar volume of *fcc* Pt as a function of pressure at 300 K (full scale with the liquid phase (a) and lower pressure region (b)). The experimental data are from Refs. [24] [70McQ], [25] [74MOR], [27] [89HOL], [18] [04DEW], [19] [04FEI], [20] [08ZHA] and [21] [19ANZ]. Calculated data are obtained in this work from PBEsol calculation.

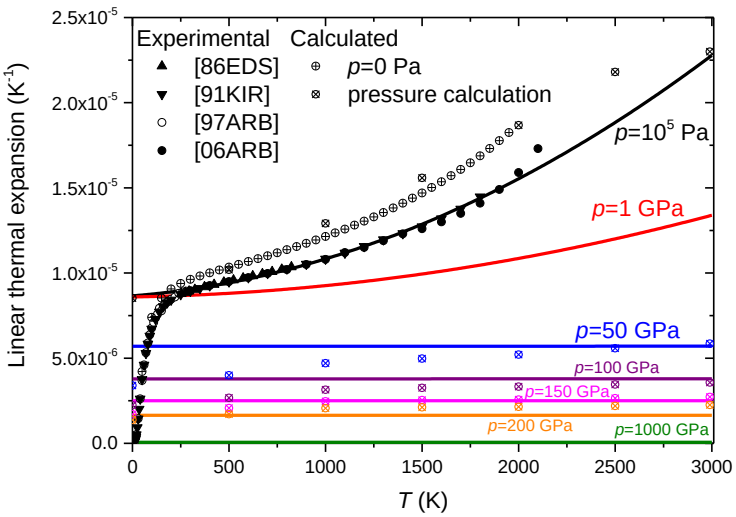


Figure 5: Linear thermal expansion of *fcc* Pt as a function of temperature for different pressures. The experimental data are from Refs. [63] [86EDS], [64] [91KIR], [13] [97ARB] and [14] [06ARB]. Calculated data are obtained in this work from PBEsol DFT and phonon calculation at zero pressure and at different pressures (see text).

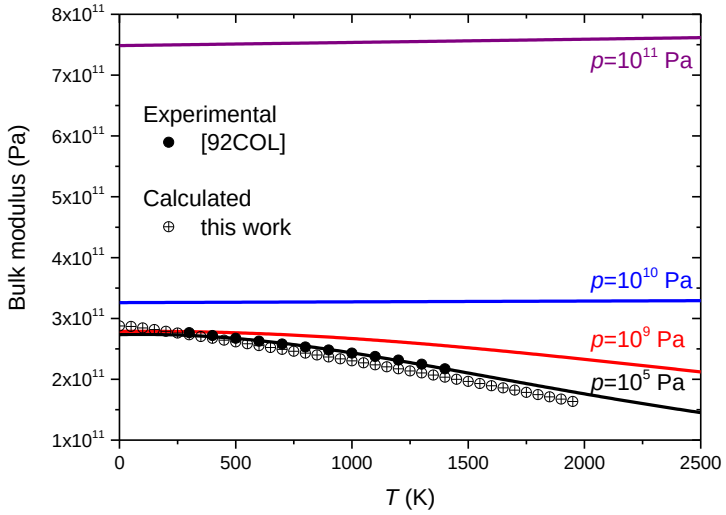


Figure 6: Bulk modulus of *fcc* Pt as a function of temperature at different pressures. The experimental data is from [28] [92COL] and has been transformed from adiabatic to isothermal bulk modulus. Calculated data are obtained in this work from PBEsol DFT and phonon calculation at zero pressure.

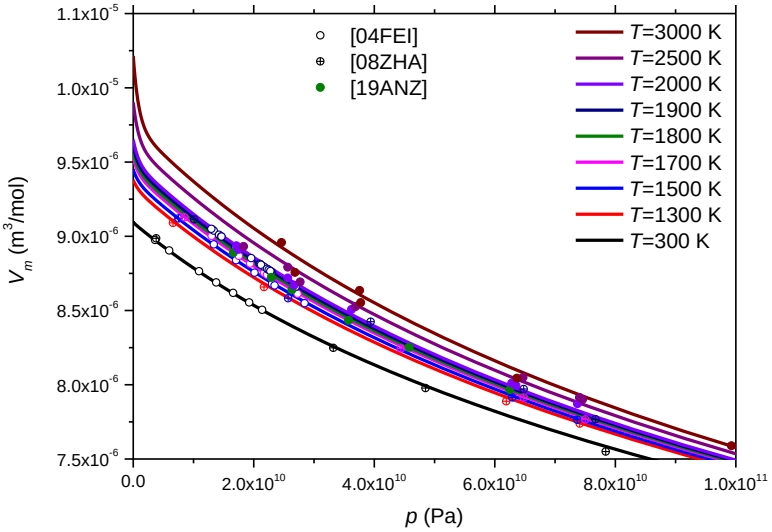


Figure 7: Molar volume of *fcc* Pt as a function of pressure at different temperatures. The experimental data are from [19] [04FEI], [20] [08ZHA] and [21] [19ANZ].

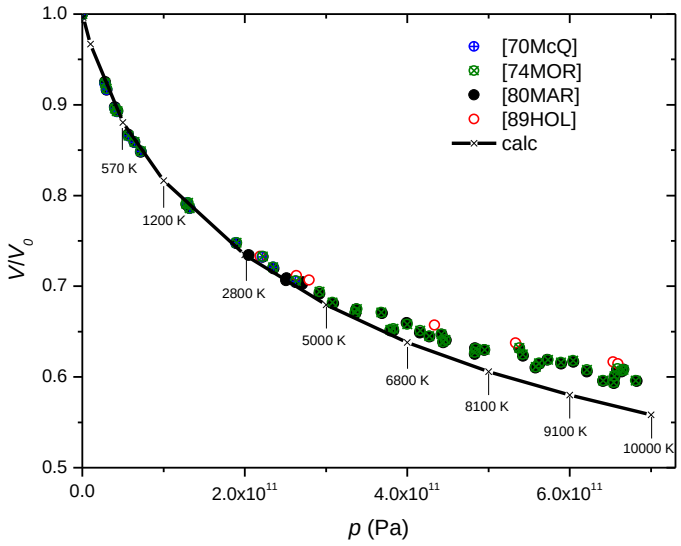


Figure 8: Hugoniot plot of *fcc* Pt with indication of the temperature at different points of the curve. The experimental data are from Refs. [24] [70McQ], [25] [74MOR], [26] [80MAR] and [27] [89HOL].

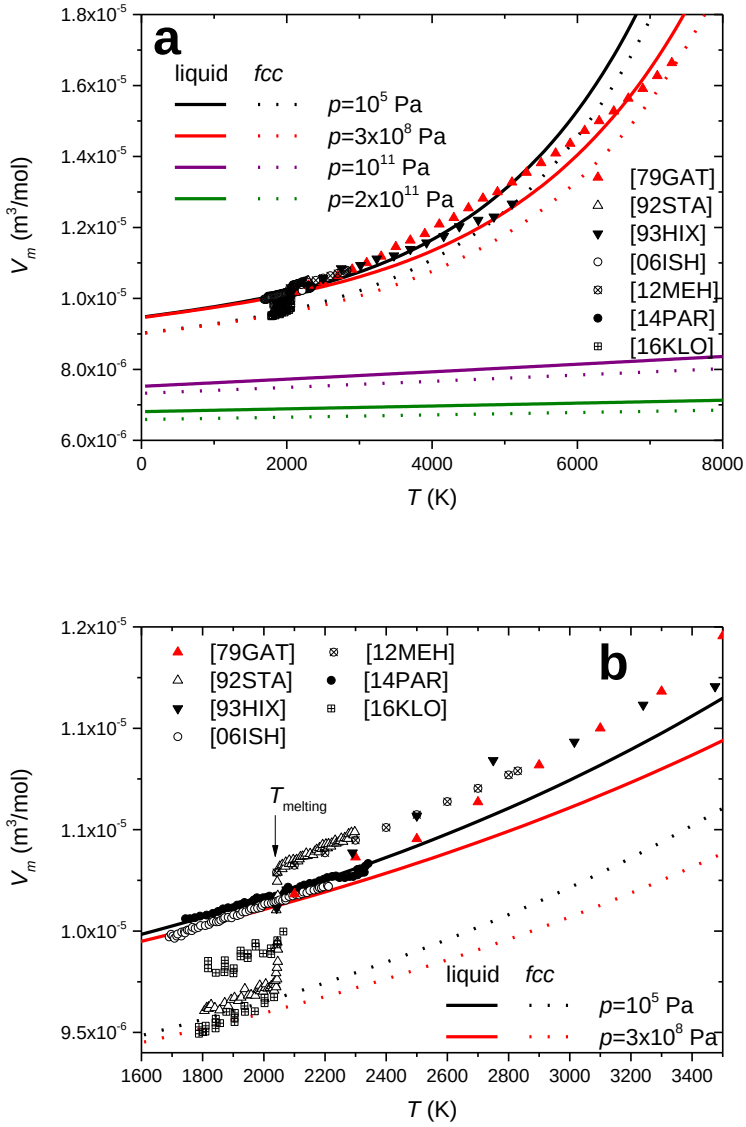


Figure 9: Molar volume of liquid Pt (*fcc* is shown for comparison) at different pressures (full scale (a) and zoom around the melting point (b)). The experimental data are from Refs. [16] [14PAR], [36] [79GAT] (at $3.10^8$ Pa), [37] [93HIX], [34] [92STA], [38] [06ISH], [15] [12MEH] and [17] [16KLO].

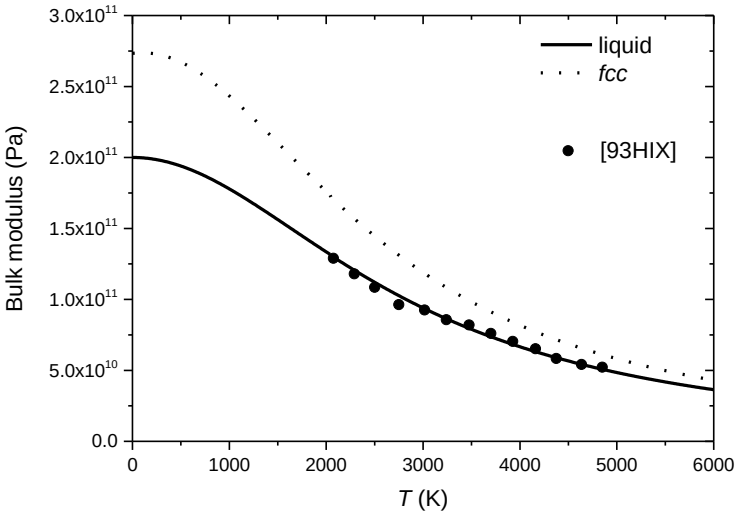


Figure 10: Bulk modulus of liquid Pt (*fcc* phase is shown for comparison) at $p$=$10^5$ Pa. Experimental data is from Ref. [37] [93HIX].

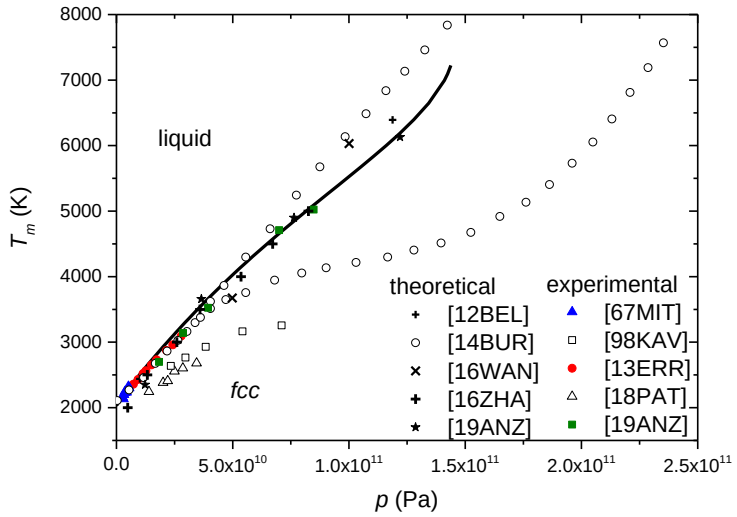


Figure 11: melting curve of Pt. Experimental data are from Refs. [41] [67MIT], [47] [98KAV], [43] [12BEL], [40] [13ERR], [44] [14BUR], [45] [16WAN], [46] [16ZHA], [48] [18PAT] and [21] [19ANZ]. The data from Ref. [44] [14BUR] above 40 GPa represent equilibrium between *hcp* and *fcc* or liquid and are not to be considered.

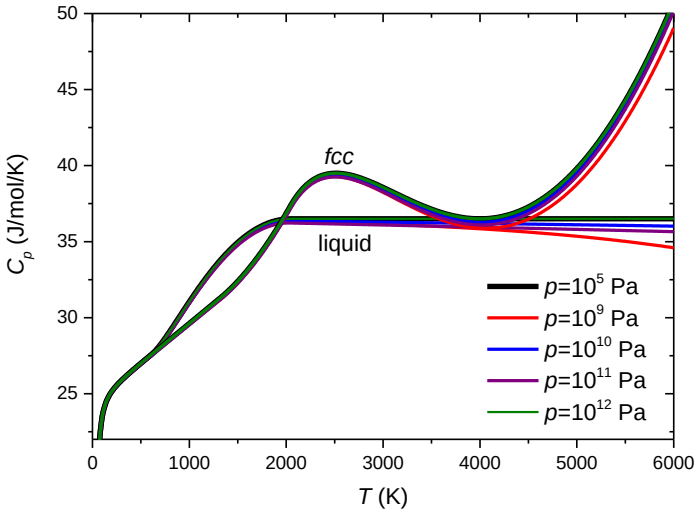


Figure 12: $C_p$ of *fcc* and liquid Pt at different pressures.

**References**


[1] M.H.G. Jacobs, H.A.J. Oonk, A realistic equation of state for solids. The high pressure and high temperature thermodynamic properties of MgO, Calphad 24 (2) (2000) 133-147.

[2] X.-G. Lu, M. Selleby, B. Sundman, Implementation of a new model for pressure dependence of condensed phases in Thermo-Calc, Comput. Coupling Phase Diagr. Thermochem. 29 (2005) 49-55.

[3] L. Stixrude, C. Lithgow-Bertelloni, Thermodynamics of mantle materials - I. Physical properties, Geophys. J. Int. 162 (2005) 610-632.

[4] M.H.G. Jacobs, A.P. van den Berg, B.H.W.S. de Jongh, The derivation of thermo-physical properties and phase equilibria of silicate materials from lattice vibrations: application to convection in the Earth's mantle, Comput. Coupling Phase Diagr. Thermochem. 30 (2006) 131-146.

[5] E. Brosh, G. Makov, R.Z. Shneck, Application of Calphad to high pressures, Comput. Coupling Phase Diagr. Thermochem. 31 (2007) 173-185.

[6] E. Brosh, R.Z. Shneck, G. Makov, Explicit Gibbs free energy equation of states for solids, J. Phys. Chem. Solids 69 (2008) 1912-1922.

[7] X.-G. Lu, Q. Chen, A CALPHAD Helmholtz energy approach to calculate thermodynamic and thermophysical properties of fcc Cu, Philos. Mag. 89 (25) (2009) 2167-2194.

[8] M.H.G. Jacobs, R. Schmid-Fetzer, Thermodynamic properties and equation of state of fcc aluminum and bcc iron, derived from a lattice vibrational method, Phys. Chem. Miner. 37 (10) (2010) 721-739.

[9] J.-M. Joubert, J.-C. Crivello, K.V. Yusenko, Modification of Lu's (2005) high pressure model for improved high pressure/high temperature extrapolations. Part II: modeling of osmium–platinum system at high pressure/high temperature, Calphad: Comput. Coupling Phase Diagrams Thermochem. submitted (2021).

[10] A. Fernández Guillermet, Critical evaluation of the thermodynamic properties of molybdenum, Int. J. Thermophys. 6 (4) (1985) 367-393.

[11] J.-O. Andersson, A. Fernández Guillermet, P. Gustafson, M. Hillert, B. Jansson, B. Jönsson, B. Sundman, J. Ågren, A new method describing lattice stabilities, Calphad 11 (1) (1987) 93-98.

[12] X.-G. Lu, M. Selleby, B. Sundman, Theoretical modeling of molar volume and thermal expansion, Acta Mater. 53 (2005) 2259-2272.

[13] J.W. Arblaster, Crystallographic properties of platinum, Platin. Met. Rev. 41 (1) (1997) 12-21.

[14] J.W. Arblaster, Crystallographic properties of platinum, Platin. Met. Rev. 50 (3) (2006) 118-119.

[15] S. Mehmood, U.E. Klotz, G. Pottlacher, Thermophysical properties of platinum-copper alloys, Metall. Mater. Trans. A 43A (2012) 5029-5037.

[16] P.-F. Paradis, T. Ishikawa, J.T. Okada, Thermophysical properties of platinum group metals in their liquid undercooled and superheated phases, Jonhson Matthey Tech. 58 (3) (2014) 124-136.

[17] U.E. Klotz, Y. Plevachuk, Thermophysical properties of platinum-rich alloys measured by sessile drop experiments, High Temp., High Press. 45 (2016) 3-20.

[18] A. Dewaele, P. Loubeyre, M. Mezouar, Equations of state of six metals above 94 GPa, Phys. Rev. B70 (2004) 094112.
[19] Y. Fei, J. Li, K. Hirose, W. Minarik, J.V. Orman, C. Sanloup, W. van Westrenen, T. Komabayashi, K.-I. Funakoshi, A critical evaluation of pressure scales at high temperatures by in situ X-ray diffraction measurements, Phys. Earth Plant. In. 143-144 (2004) 515-526.
[20] C.-S. Zha, K. Mibe, W.A. Bassett, O. Tschauner, H.-K. Mao, R.J. Hemley, P-V-T equation of state of platinum to 80 GPa and 1900 K from internal resistive heating/X-ray diffraction measurements, J. Appl. Phys. 103 (2008) 054908.
[21] S. Anzellini, V. Monteseguro, E. Bandiello, A. Dewaele, L. Burakovsky, D. Errandonea, In situ characterization of the high pressure-high temperature melting curve of platinum, Sci. Rep.-UK 9 (2019) 13034.
[22] M. Matsui, E. Ito, T. Katsura, D. Yamazaki, T. Yoshino, A. Yokoyama, K.-I. Funakoshi, The temperature-pressure-volume equation of state of platinum, J. Appl. Phys. 105 (2009) 013505.
[23] Xiaoli Huang, Frangfei Li, Qiang Zhou, Gang Wu, Yanping Wang, Lu Wang, Bingbing Liu, Tian Cui, In situ synchrotron X-ray diffraction with laser-heated diamond anvil cells study of Pt up to 95 GPa and 3150 K, RSC Advances 5 (2015) 14603-14609.
[24] R.G. McQueen, S.P. Marsh, J.W. Taylor, J.N. Fritz, W.J. Carter, The equation of state of solids from shock wave studies, in High Velocity Impact Phenomena, 1970, Academic Press, 293-417.
[25] J.A. Morgan, The equation of state of platinum to 680 GPa, High Temp., High Press. 6 (1974) 195-201.
[26] S.P. Marsh. LASL shock Hugoniot data, University of California Press, 1980.
[27] N.C. Holmes, J.A. Moriarty, G.R. Gathers, W.J. Nellis, The equation of state of platinum to 660 GPa (6.6 Mbar), J. Appl. Phys. 66 (7) (1989) 2962-2967.
[28] S.M. Collard, R.B. McLellan, High-temperature elastic constants of platinum single crystals, Acta Metall. Mater. 40 (4) (1992) 699-702.
[29] E. Menéndez-Proupin, A.K. Sing, Ab initio caculations of elastic properties of compressed Pt, Phys. Rev. B76 (2007) 054117.
[30] T. Sun, K. Umemoto, Z. Wu, J.-C. Zheng, R.M. Wentzcovitch, Lattice dynamics and thermal equation of state of platinum, Phys. Rev. B78 (2008) 024304.
[31] N. Bourgeois, J.-C. Crivello, A. Saengdeejing, Y. Chen, P. Cenedese, J.-M. Joubert, Thermodynamic modeling of the Ni-H system, J. Phys. Chem. C 119 (2015) 24546-24557. https://doi.org/10.1021/acs.jpcc.5b06393.
[32] J.P. Perdew, K. Burke, M. Ernzerhof, Generalized gradient approximation made simple, Phys. Rev. Lett. 77 (18) (1996) 3865-3868. https://doi.org/10.1103/PhysRevLett.77.3865.
[33] J.P. Perdew, A. Ruzsinszky, G.I. Csonka, O.A. Vydrov, G.E. Scuseria, L.A. Constantin, X. Zhou, K. Burke, Restoring the density-gradient expansion for exchange in solids and surfaces, Phys. Rev. Lett. 100 (2008) 136406.
[34] S.V. Stankus, R.A. Khairulin, Measurement of the thermal properties of platinum in the temperature interval 293-2300 K by the method of penetrating radiation, High Temp. 30 (3) (1992) 386-391.
[35] G.R. Gathers, J.W. Shaner, W.M. Hodgson, Thermodynamic characterization of liquid metals at high temperature by isobaric expansion measurements, Lawrence Livermore Laboratory, Report UCRL-80114, 1978.
[36] G.R. Gathers, J.W. Shaner, W.M. Hodgson, Thermodynamic characterization of liquid metals at high temperature by isobaric expansion measurements, High Temp., High Press. 11 (1979) 539-538.
[37] R.S. Hixson, M.A. Winkler, Thermophysical properties of liquid platinum, Int. J. Thermophys. 14 (3) (1993) 409-416.
[38] T. Ishikawa, P.-F. Paradis, N. Koike, Non-contact thermophysical property measurements of liquid and supercooled platinum, Jpn. J. Appl. Phys 45 (3A) (2006) 1719-1724.

[39] J.W. Arblaster, Selected values for the densities and molar volumes for the platinum group metals and of the initial melting curves of iridium, rhodium and ruthenium, Jonhson Matthey Tech. 61 (2) (2017) 81-87.
[40] D. Errandonea, High-pressure melting curves of the transition metals Cu, Ni, Pd, and Pt, Phys. Rev. B87 (2013) 054108.
[41] N.R. Mitra, D.L. Decker, H.B. Vanfleet, Melting curves of copper, silver, gold, and platinum to 70 kbar, Phys. Rev. 161 (3) (1967) 613-617.
[42] L.F. Vereshchagin, N.S. Fateeva, Melting curves of graphite, tungsten, and platinum up to 60 kbar, JETP 28 (4) (1969) 597-600.
[43] A.B. Belonoshko, A. Rosengren, High-pressure melting curve of platinum from ab initio Z method, Phys. Rev. B85 (2012) 174104.
[44] L. Burakovsky, S.P. Chen, D.L. Preston, D.G. Sheppard, Z methodologies for phase diagram studies: platinum and tantalum as examples, Journal of Physics: Conference Series 500 (2014) 162001.
[45] Pan-Pan Wang, Ju-Xiang Shao, Qi-Long Cao, Melting properties of Pt and its transport coefficients in liquid states under high pressure, Int. J. Mod. Phys. 30 (1) (2016) 1550250.
[46] Baoling Zhang, Baowen Wang, Qingxin Liu, Melting curves of Cu, Pt, Pd, and Au under high pressures, Int. J. Mod. Phys. 30 (2016) 1650013.
[47] A. Kavner, R. Jeanloz, High-pressure melting curve of platinum, J. Appl. Phys. 83 (12) (1998) 7553-7559.
[48] N.N. Patel, M. Sunder, High pressure melting curve of platinum up to 35 GPa, AIP Conf. Proc. 1942 (2018) 030007.
[49] P.I. Dorogokupets, A.R. Oganov, Ruby, metals, and MgO as alternative pressure scales: a semiempirical description of shock-wave, ultrasonic, x-ray, and thermochemical data at high temperatures and pressures, Phys. Rev. B75 (2007) 024115.
[50] A. Karbasi, S.K. Saxena, R. Hrubiak, The thermodynamics of several elements at high pressure, Calphad: Comput. Coupling Phase Diagrams Thermochem. 35 (2011) 72-81.
[51] M.H.G. Jacobs, R. Schmid-Fetzer, A.P. van den Berg, An alternative use of Kieffers's lattice dynamics model using vibrational density of states for constructing thermodynamic databases, Phys. Chem. Miner. 40 (2013) 207-227.
[52] Zhifeng Xu, Xin Guo, Xiao-Gang Lu, Study of thermodynamic and thermophysical properties of fcc Pt through CALPHAD approach, Shanghai Met. 038 (6) (2016) 71-76.
[53] Y. Fei, E. Brosh, Experimental study and thermodynamic calculations of phase relations in the Fe-C system at high pressure, Earth Planet. Sc. Lett. 408 (2014) 155-162.
[54] D. Huang, S. Liu, Y. Du, B. Sundman, Modeling of the molar volume of the solution phases in the Al-Cu-Mg system, Calphad: Comput. Coupling Phase Diagrams Thermochem. 51 (2015) 261-271.
[55] B. Sundman, P. Shi. SGTE Pure Element Database, version 5.1, Stockholm: Thermo-Calc Software, 2002.
[56] S. Bigdeli, L.-F. Zhu, A. Glensk, B. Grabowski, B. Lindahl, T. Hickel, M. Selleby, An insight into using DFT data for Calphad modeling of solid phases in the third generation of Calphad databaes, a case study for Al, Calphad 65 (2019) 79-85.
[57] M. Schick, A. Watson, M. to Baben, K. Hack, A modified Neumann-Kopp treatment of the heat capacity of stoichiometric phases for use in computational thermodynamics, J. Phase Equilibr. Diffus. 40 (2019) 104-114.
[58] B. Sundman, U.R. Kattner, M. Hillert, J. Ågren, S. Bigdeli, Q. Chen, A. Dinsdale, B. Hallstedt, A. Khvan, H. Mao, R. Otis, A method for handling the extrapolation of solid crystalline phases to temperature far above their melting point, Calphad: Comput. Coupling Phase Diagrams Thermochem. 68 (2020) 101737.
[59] T. Hammerschmidt, I.A. Abrikosov, D. Alfè, S.G. Fries, L. Höglund, M.H.G. Jacobs, J. Kossmann, X.-G. Lu, G. Paul, Including the effects of pressure and stress in thermodynamic functions, Phys. Status Solidi (b) 251 (1) (2014) 81-96.

[60] H. Kangarlou, A. Abdollahi, Thermodynamic properties of copper in a wide range of pressure and temperature within the quasi-harmonic approximation, Int. J. Thermophys. 35 (2014) 1501-1511.
[61] M. Tirone, On the use of thermal equations of stateand the extrapolation at high temperature and pressure for geophysical and petrological applications, Geophys. J. Int. 202 (2015) 1483-1494.
[62] J.W. Edwards, R. Speiser, H.J. Johnston, High temperature structure and thermal expansion of some metals as determined by X-ray diffraction data. I. Platinum, Tantalum, Niobium, and Molybdenum, J. Appl. Phys. 22 (4) (1951) 424-428.
[63] R.E. Edsinger, M.L. Reilly, J.F. Schooley, Thermal expansion of platinum and platinum-rhodium alloys, J. Res. Nat. Bur. Stand. 91 (6) (1986) 333-356.
[64] R.K. Kirby, Platinum-A thermal expansion reference material, Int. J. Thermophys. 12 (4) (1991) 679-685.

Supplementary materials to:

Modification of Lu's (2005) high pressure model for improved high pressure/high temperature extrapolations. Part I: modeling of platinum at high pressure/high temperature

Jean-Marc Joubert[1], Jean-Claude Crivello[1]

[1]Univ Paris Est Creteil, CNRS, ICMPE, UMR 7182, 2 rue Henri Dunant, 94320 Thiais, France

e-mail address of corresponding author: joubert@icmpe.cnrs.fr

## 1. Comparison of the three functionals used for the DFT calculation of *hcp* Os

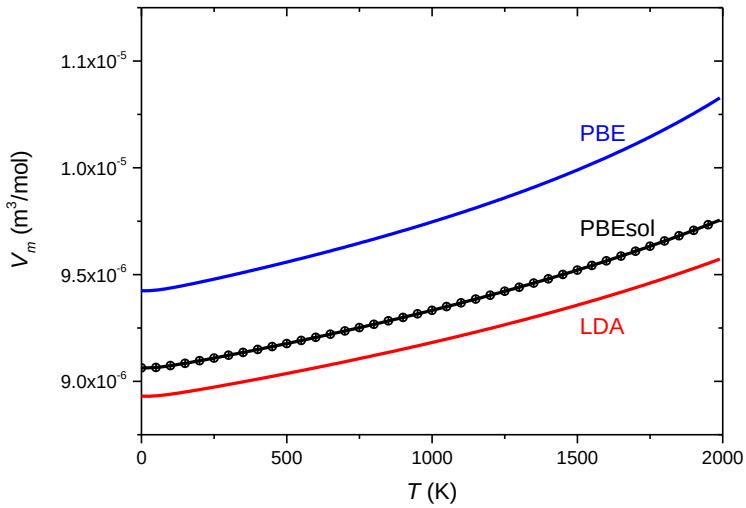


Figure 1: Molar volume of *fcc* Pt as a function of temperature calculated with three different functionals.

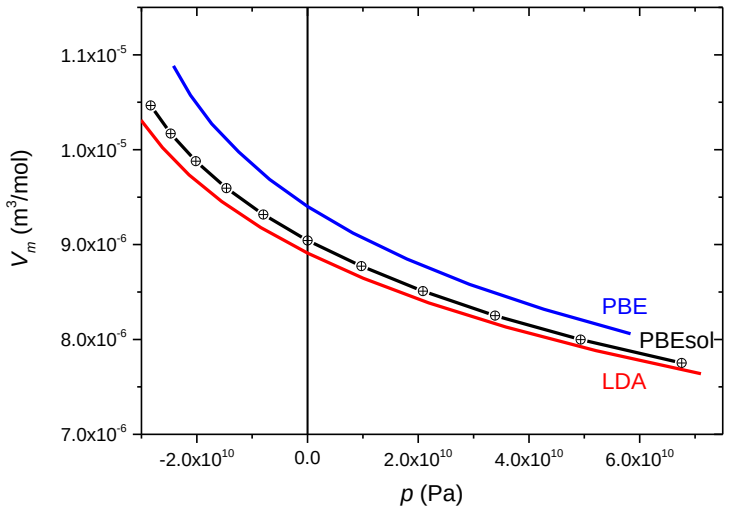


Figure 2: Molar volume of *fcc* Pt as a function of pressure at 0 K calculated with three different functionals.

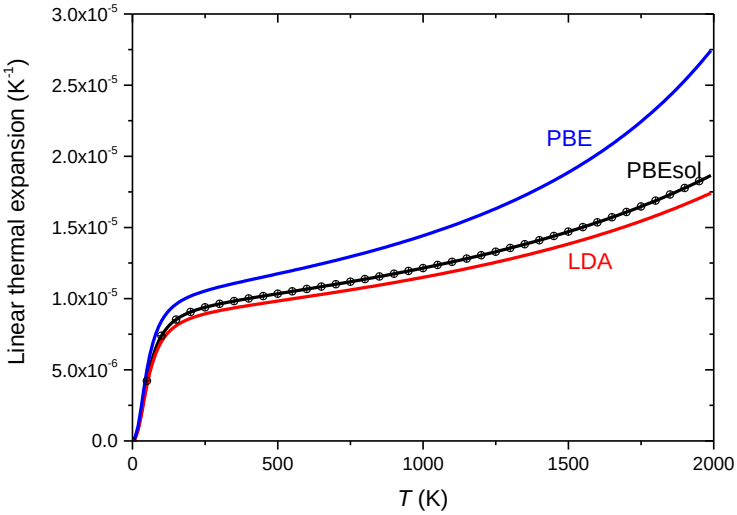


Figure 3: Linear thermal expansion of *fcc* Pt as a function of temperature calculated with three different functionals.

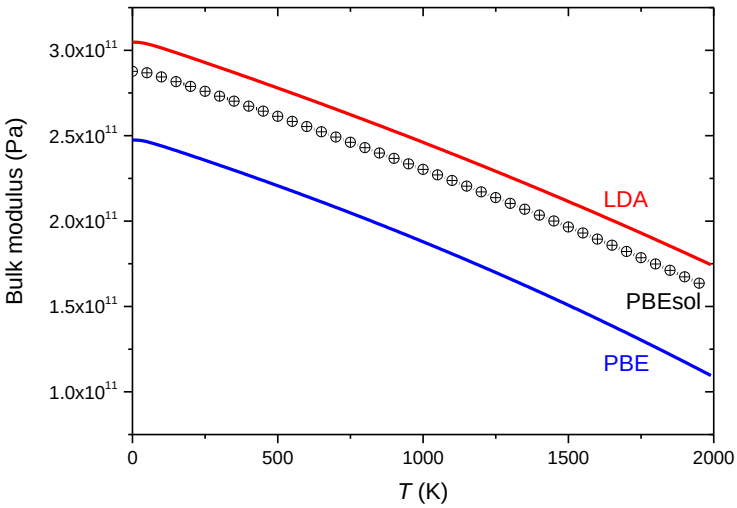


Figure 4: Bulk modulus of *fcc* Pt as a function of temperature calculated with three different functionals.

```
$ Pt system at high pressure


$ Database file written 2020-12- 4
$ From database: User data 2020.05.14
 ELEMENT /-   ELECTRON_GAS              0.0000E+00  0.0000E+00  0.0000E+00!
 ELEMENT VA   VACUUM                    0.0000E+00  0.0000E+00  0.0000E+00!
 ELEMENT PT   UNKNOWN                   0.0000E+00  0.0000E+00  0.0000E+00!


 FUNCTION GHSERPT   298.15 -7595.631+124.388275*T-24.5526*T*LN(T)
     -.00248297*T**2-2.0138E-08*T**3+7974*T**(-1); 1300 Y
      -9253.174+161.529615*T-30.2527*T*LN(T)+.002321665*T**2
     -6.56946E-07*T**3-272106*T**(-1); 2041.50 Y
      -222048.216+1019.35892*T-136.192996*T*LN(T)+.020454938*T**2
     -7.59259E-07*T**3+71539020*T**(-1); 4000 N !
 FUNCTION GLIQPT    298.15 +12518.385+115.113092*T-24.5526*T*LN(T)
     -.00248297*T**2-2.0138E-08*T**3+7974*T**(-1); 600 Y
      +19023.491+32.94182*T-12.3403769*T*LN(T)-.011551507*T**2
     +9.31516E-07*T**3-601426*T**(-1); 2041.50 Y
      +1404.468+205.858962*T-36.5*T*LN(T); 4000 N !
 FUNCTION F11       100 -1.0000000000000000E-009*P; 3000 N !
 FUNCTION EXPO1     100 +1*EXP(F11#); 3000 N !
 FUNCTION F12       100 -9.048576980000000E-012*P; 3000 N !
 FUNCTION EXPO2     100 +1*EXP(F12#); 3000 N !
 FUNCTION UN_ASS 298.15 +0; 300 N !

 TYPE_DEFINITION % SEQ *!
 DEFINE_SYSTEM_DEFAULT ELEMENT 2 !
 DEFAULT_COMMAND DEF_SYS_ELEMENT VA /- !


 TYPE_DEFINITION & GES A_P_D FCC_A1 MAGNETIC  -3.0    2.80000E-01 !
 PHASE FCC_A1  %&  2 1   1 !
    CONSTITUENT FCC_A1  :PT : VA :  !

   PARAMETER G(FCC_A1,PT:VA;0)            298.15 +GHSERPT#; 4000 N REF0 !
   PARAMETER V0(FCC_A1,PT:VA;0)           298.15 9.02040956E-006;
   6000 N REF0 !
   PARAMETER VA(FCC_A1,PT:VA;0)           298.15 2.59775898E-005*T*EXPO2#
+1.353321440000000E-009*T**2*EXPO1#+1.26832868E-012*T**3*EXPO1#; 6000 N REF0 !
   PARAMETER VC(FCC_A1,PT:VA;0)           298.15 1.68443528E-006; 6000 N REF0 !
   PARAMETER VK(FCC_A1,PT:VA;0)           298.15 3.65798657E-012
   -1.08751254E-016*T*EXPO1#
  +5.602994870000000E-019*T**2*EXPO1#; 6000 N REF0 !


 PHASE LIQUID  %  1  1.0  !
    CONSTITUENT LIQUID  :PT :  !

   PARAMETER G(LIQUID,PT;0)               298.15 +GLIQPT#; 5500 N REF0 !
   PARAMETER V0(LIQUID,PT;0)              298.15 9.468684986996620E-006;
   6000 N REF0 !
   PARAMETER VA(LIQUID,PT;0)         298.15 2.954623283520561E-005*T*EXPO2#
  +1.397638283912732E-012*T**3*EXPO1#; 6000 N REF0 !
   PARAMETER VC(LIQUID,PT;0)              298.15 1.440924031148858E-006;
   6000 N REF0 !
   PARAMETER VK(LIQUID,PT;0)              298.15 5.0E-012
  +6.226567975868238E-019*T**2*EXPO1#; 6000 N REF0 !

 LIST_OF_REFERENCES
 NUMBER  SOURCE
  !
```